Characterization of mechanical behaviour of aluminum powders under fast dynamic conditions

Francesco Delloro[1*], *Hugo* Durand[1], *Laurent* Lacourt[1], *Jean-Christophe* Teissedre[1], *Alain* Thorel[1], *Imène* Lahouij[2], *François* Lavaud[3] and *Xavier* Clausse[3]

[1] MINES ParisTech, PSL Research University, MAT – Centre des Matériaux, CNRS UMR 7633, BP 87, 91003 Evry, France
[2] MINES ParisTech, PSL Research University, CEMEF – Centre de Mise en Forme des Matériaux, CNRS UMR 7635, - 06904 Sophia Antipolis cedex
[3] TOYAL EUROPE, Route de Lescun F-64490 Accous, France

Abstract. Cold spray is a process belonging to the thermal spray family, characterized by relatively low temperatures and high particle velocities. Upon impact, particles undergo large plastic deformation at solid state in dynamic regime up to 10^9 s^{-1}. The knowledge of powder behaviour in such conditions is essential to catch key phenomena in cold spray and a necessary step for a correct process modelling. However, little is known on mechanical behaviour of feed-stock powders when submitted to cold spray conditions. In this study, an approach focused on single particles combining laser shock induced impact, namely LASHPOL (LAser SHock POwder Launcher), and quasi-static compression was therefore developed. This method was applied in this study on spherical Aluminium powders but can work with any other powder material. The mechanical behaviour of powders was characterized and used to fit the parameters of Johnson-Cook constitutive model, by means of finite element inverse method. The combination of static and dynamic tests resulted in an original characterization of powder, which revealed having a different mechanical behaviour than the corresponding bulk material.

Table 1. List of acronyms.

Acronym	Name
BSE	Back Scattered Electrons
CEL	Coupled Eulerian Lagrangian
FEM	Finite Element Method
JC	Johnson-Cook
LASHPOL	LAser SHock POwder Launcher
SEM	Scanning Electron Microscope

* Corresponding author: francesco.delloro@mines-paristech.fr

1 Introduction

Cold spray is an additive process where the feed-stock material is a dry powder. Particles are accelerated by a supersonic gas at high velocities, while temperature is kept relatively low. When impacting with the substrate, particles undergo large plastic deformation in a rapid dynamic regime (locally up to 10^9 s^{-1}) [1]. Material deposition is the result of the stacking of impinging particles. This process, discovered in the 80's, is the object of a growing interest from the academic and industrial worlds due to its versatility allowing numerous applications, from repair to functional coating and additive manufacturing.

The simulation of particle impact is key to understand coating build-up mechanisms, in view of process optimization and prediction of final coating properties. Independently of the constitutive model, parameter values available in literature are mostly fitted from Split-Hopkinson pressure bar experiments, giving access at considerably lower strain rates (10^5 s^{-1} at best) [2]. In addition, most of these results are originated from bulk samples, several orders of magnitude bigger than cold spray powders. Atomized powders, when compared to bulk materials, are characterized by finer grain sizes due to the high cooling rates involved in the atomization process [3-4]. Mechanical behaviour, which is well known to be microstructure-dependent, can thus be expected to be different from powder to bulk material. To improve cold spray process modelling and open the way for its predictability, new methods for mechanical characterization of powders are needed.

The mechanical wave generated by a pulsed laser in the nanosecond regime [5, 6] can be used to accelerate single particles at speeds in the same order as in cold spray, thus realizing an experimental simulation of the process in precisely controlled conditions. This would not be possible during the process itself, due to the large number (> 10^6 s^{-1}) of particles and the variability in their velocities and sizes. Hassani *et al.* [7, 8] already developed a similar experimental method and compared with FEM simulation, showing the possibility of fitting material model parameters. Nevertheless, the simultaneous fitting of all the unknown parameters of the constitutive model seems difficult to perform with a single experimental data set. Other experimental frameworks can be used to gather different material behaviour data. A work in this direction [9] developed a single particle compression test, realized by a nanoindentation system equipped with a flat head. The device could measure force and displacement, generating data that could be compared with FEM results, allowed the fitting of a constitutive model. Nevertheless, effects due to substrate roughness were not taken in account and the fitting procedure was based on some hypothesis.

In the present work, a quasi-static single particle compression test was developed, taking advantage of a SEM *in-situ* nanoindentation stage with a flat head. In parallel, single particle micro-ballistic experiments were developed. FE modelling of these two tests and the use of Kriging methods allowed to fit constitutive model parameters for powders. Moreover, the same methods allowed beginning to study the dependency of material properties on particle size, composition and atomizing conditions. Indeed, powders produced by atomization typically come in a wide range of sizes (typically 1 to 100 µm). Even if particle size distribution is narrowed by sieving, there still remains a considerable range of size variation in a cold spray powder batch. Given that solidification rate during atomization is related to particle size, microstructure and mechanical properties are expected to vary among particles within the same batch.

The Johnson-Cook model (JC in the following) [10], in Eq. 1, is widely used for the material behaviour for cold spray simulation and had been chosen for this study for the sake of simplicity. Nevertheless, the method developed in the present work can be applied to any constitutive model, such as, for example, the PTW model [11] for metals or other for polymers [7], [12-14] .

$$\sigma = \left(A + B\,\varepsilon_p^n \right) \left[1 + C\ log\left(\frac{\dot{\varepsilon}_p}{\dot{\varepsilon}_0} \right) \right] \left[1 - \left(\frac{T - T_{ref}}{T_{melt} - T_{ref}} \right)^m \right] \quad (1)$$

where σ is the yield stress, A, B, n, C and m are materials parameters, ε_p is the equivalent plastic strain and $\dot{\varepsilon}_p$ is the equivalent plastic strain rate, $\dot{\varepsilon}_0$ is a reference strain rate, T is the actual temperature, T_{ref} is a reference temperature, T_{melt} is the melting temperature. The yield stress is the product of three factors, representing, respectively from left to right in Eq. 1, strain hardening, strain rate hardening and thermal softening.

The present work, joining experimental and numerical techniques, brings into play accurate mechanical characterization methods, specific to powder materials. Powder mechanical properties in static and dynamic conditions can then be tested, independently of long and costly cold spraying experiments. This will, on one hand, deepen the knowledge on powder materials which are more and more used in industry and, on the other hand, greatly help in accelerating powder optimization process for given applications, as for example cold spray of aluminium alloys onto different substrates.

2 Materials and methods

In this study a particular Al powder produced by Toyal Europe (Accous, France), the 1070-B5 (composition >99.7% Al, 0.09% Fe and 0.04% Si), was chosen for its almost-perfectly spherical shape, making it an ideal candidate for the comparison of experimental results with numerical simulations. Size distribution had a d_{50} of 53 µm.

The quasi-static test consisted in applying compression loadings on single particles. To this aim, a SEM equipped with in-situ nano-indentation stage, namely the ASA (Alemnis Standard Assembly) by Alemnis (Thun, Switzerland), was used. Force-displacement data were acquired by a static sensor at 10 Hz calibrated up to 0.5 N in force and with sensitivity in the nm scale. A diamond punch with a flat head of 116 µm diameter applied the load to the particle. Mirror-polished sapphire was used as a substrate. The choice of substrate and indenter materials, with very high Young modulus, was important to get rid of parasitic elastic effects and allowed to avoid corrections on measured deformations. Using an ethanol-based dispersion and a micropipette, less than 15 particles could be deposited on a Sapphire substrate, separated each other by a distance of few hundreds microns to avoid any interference. A 8 nm platinum layer was applied to avoid charging effect from SEM electron beam.

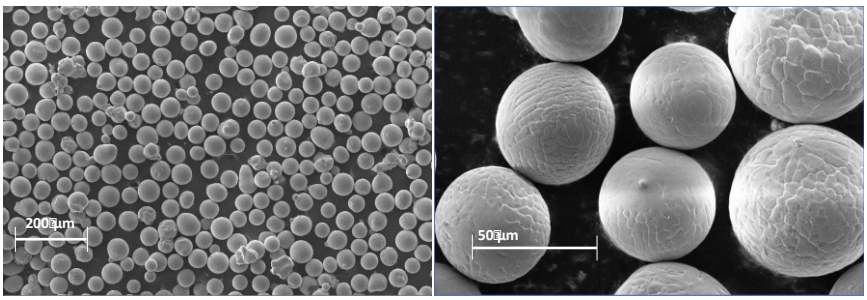

Fig. 1. SEM BSE image of Al 1070-B5 powder, at different magnifications..

The LASHPOL stage was designed with the purpose of accelerating a single particle to measurable velocities in the 100-1000 m.s^{-1} range. The pulsed laser source was a SAGA 330 by Thalès (Courbevoie, France), with 2 J maximum energy and pulse duration about 5 ns. Single particles were deposited onto the launcher substrate, an appositely conceived

multi-layer multi-material sheet assembly. The pulsed laser illuminated the launcher back face creating a plasma whose expansion could rapidly deform the launcher and accelerate the particle. The latter flew less than two cm before impacting a receiver substrate (an aluminum sheet in the present work). Particle velocities depended on laser energy and spot diameter. Particle velocity and trajectory were acquired using a high-speed imaging system made by a SA 1.1 camera from Photron (Tokyo, Japan), operating at 180 kHz with a field of view of 14.3 x 1.5 mm^2, and an illuminating pulsed laser Cavilux HF, from Cavitar (Tampere, Finland), synchronized with the camera. In LASHPOL experiments, particle diameter was measured before the test with an optical microscope VHX from KEYENCE (Osaka, Japan). After the impact, splats were observed by high resolution SEM SEMDSM982 Gemini from ZEISS (Oberkochen, Germany).

3 Results and discussion

3.1 Single particle micro-compression

Quasi-static mechanical behavior of particles was assessed by single particle micro-compressions. First, the contact between the flat-punch and the isolate particle was set, as shown in Fig.2, on the top, where a spherical particle is positioned between the substrate and the indenter head. To assure quasi-static conditions, the loading rate was set at 0.1 $mN.s^{-1}$. Upper load limits were chosen in function of particle diameters to avoid an excessive deformation, which could result in particle sticking to the flat-punch and a consistent loss of time due to a complex cleaning procedure.

The choice of a highly spherical powder morphology allowed a consistent simplification in modelling. Nevertheless, Hertz's contact theory, giving an analytical solution to the sphere/plane contact, could not be applied due to consistent local plastic deformations that, according to [15], would appear in early deformation stages, well below the sensitivity of the experimental system. Instead, a FEM 2D axisymmetric model was developed on Abaqus/Standard® commercial software. The different size of each particle made difficult a direct comparison between experiments. For each particle, therefore, experimental force-displacement data could be compared to modelling results and be used to fit the three static JC parameters A, B and n (Eq. 1). Taking advantage of the symmetry of the problem, a particle quarter was sufficient as simulation domain. The diamond flat punch was modelled as a rigid-body and simulations were displacement-driven. Normal contact with the "hard" option was set between the particle and the flat punch and a Coulomb friction model with penalty formulation was chosen for the tangential part. The friction coefficient was set to 1.4 for all simulations. The following material parameters were used: Young modulus 70 GPa, Poisson ratio 0.27, mass density 2790 $kg.m^{-3}$.

A preliminary mesh convergence study, not reported here for brevity, resulted in an optimal mesh size of d/120, with d the particle diameter. "Hybrid" elements were used to avoid hourglass effect and enhance simulation convergence.

Static JC parameters (A, B and n) were varied around literature values [16], as shown in Table 2. The optimization problem consisting in finding the parameter set giving the best fit with experiments was solved using a kriging metamodel, capable of predicting a microcompression curve given any set of input parameters (A, B and n) inside its training range, shown in Table 2. The kriging model allowed a "virtual" computation 120 000 times faster than a FE Abaqus analysis. Finally, the optimized set of JC parameters obtained by the kriging method was validated by a FEM Abaqus analysis.

Table 2. Simulation parameters.

Parameter	**Literature value** [15]	**Range for kriging modeling**	**Definition**
A [MPa]	120	10-150	Initial yield stress
B [MPa]	426	50-320	Strain hardening
n [ ]	0.34	0-1	

As shown in fig. 2, the proposed method could efficiently perform a good fit of static J-C parameters. The experimental curve begins with a steep increase in force, changing than to a different slope. This trend could never be reproduced by simulation and was thus ascribed to particle pre-deformation due to transportation or due the first contact with the flat punch. It can also be noticed that FEM simulated curve was not perfectly smooth. These "steps" corresponded to nodes coming into contact with the indenter during particle compression. Finer mesh could alleviate this issue, at the price of much longer computational times. Instead, the solution retained was to apply a smoothing algorithm to the curve before feeding it to the kriging model.

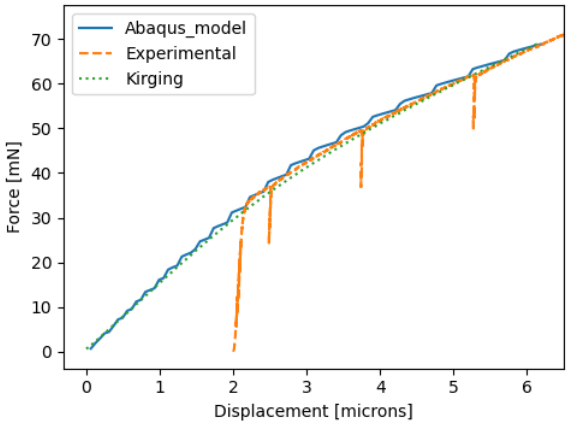

Fig. 2. Force-displacement curves. blue line: Abaqus model; orange line: experimental data; green dotted line: kriging model.

The procedure was applied to different particles, with varying sizes. For each one, a different best fitting parameter set was found, as reported in Figure 3. Values resulting from experiments (points in the graph) are quite different than literature results (lines), that are systematically obtained from Hopkinson pressure bar tests. It appears that powder material is softer than the corresponding bulk one and less sensitive to strain hardening. The powder studied was produced with a specific and confidential atomization process by Toyo Japan, to obtain its remarkable spherical shape. This unconventional production process is probably at the origin of the observed powder mechanical behaviour.

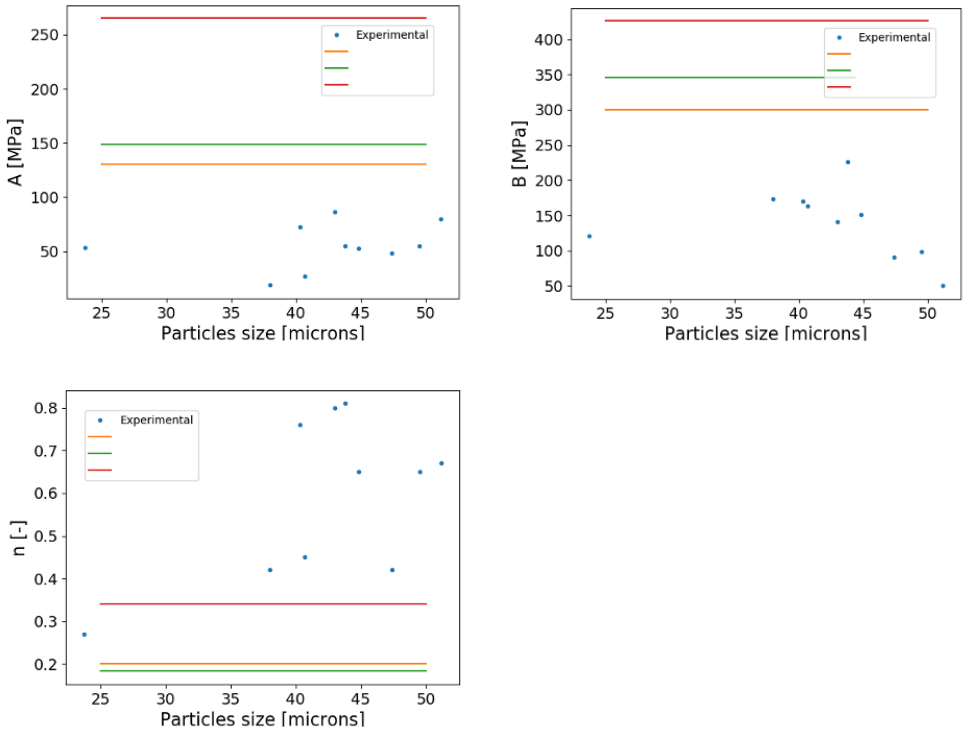

Fig. 3. Best fitting parameters as a function of particle size. Points represent values obtained in this study for different powders. Lines report literature values, from [17-19].

3.2 LASHPOL

The LASHPOL test platform was built to study particle mechanical behaviour in a very high strain rate regime. A procedure involving ethanol dispersed powder and a micropipette allowed depositing a single particle onto a specific substrate, called the launcher. A 250 µm thick Al sheet was chosen as receiver substrate.

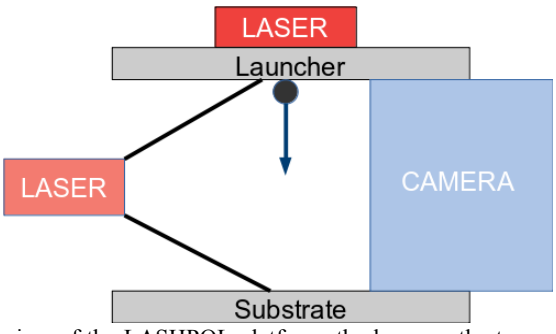

Fig. 4. Schematic view of the LASHPOL platform: the laser on the top generates the shock, the one on the left illuminates flying particles.

The LASHPOL platform was equipped with an high-speed imaging system. The camera and the light source were in front of each other, so that flying particles masked some parts

of the CCD detector. In recorded images, as illustrated in Fig. 5, particles appeared as black dots on a brighter background. The Cavilux laser flash had a 50 ns pulse duration, short enough to avoid blurred trails on camera images. Spatial resolution was calibrated placing an object of precise and known size in the camera field. Particle velocities were then obtained measuring the distance travelled between successive camera frames, as shown in Fig. 5, knowing the time interval between them.

An optical microscope was used to measure particle size before the test. After the test, deformed particles, namely splats, were observed by SEM, as shown in Fig. 6. Here, splat diameter measured 61.9 µm. Both particle and substrate underwent severe deformations at impact. Some jetting could be observed as well.

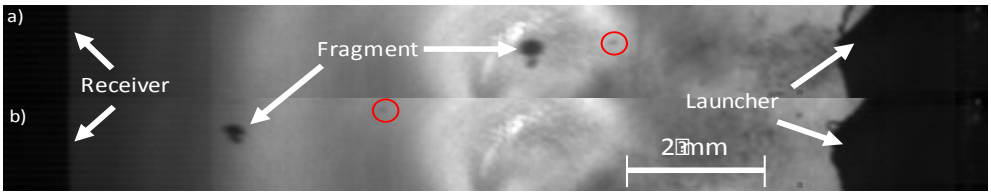

Fig. 5. Two images recorded in LASHPOL experiments. The launcher is on the right and the receiver on the left. The particle is highlighted by a circle and a detached launcher fragment by white arrows. a) 2nd frame recorded (5.5 µs after the laser shock), b) 3rd frame recorded (11.1 µs after the laser shock).

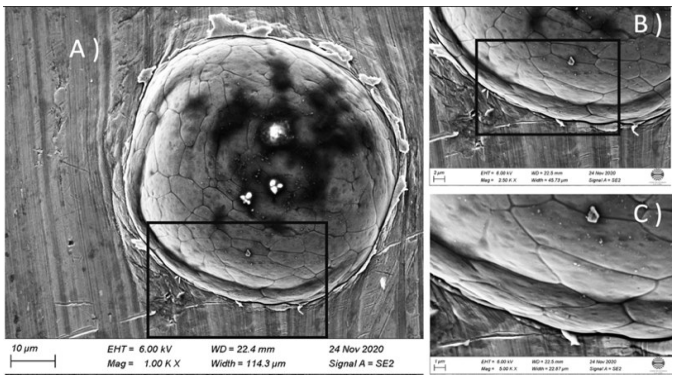

Fig. 6. SEM images with BSE detector of Al splat LASHPOL'ed at 675m.s^{-1} onto a Al sheet. a), b) and c), top views at different magnifications

The three static coefficients, A, B and n, were fixed with the micro-compression test. To fit the two remaining JC coefficients, the strain rate factor C and the thermal softening exponent m, particle impacts were modeled by FEM. Again, particles were assimilated to spheres. Due to large deformations at impact, a CEL (Coupled Eulerian Lagrangian) approach was chosen, based on the work of [20]. The particle was defined in a fixed Eulerian domain, while the receiver substrate in a Lagrangian one. Particle initial velocity and temperature were set to the experimentally measured values of, respectively, 820 m.s^{-1} and 20°C. JC model (Eq. 1) and a Mie-Grüneisen equation of state in the Us-Up formulation (Eq. 2) were chosen as substrate and particle material constitutive models.

$$p - p_H = \Gamma \rho \left(E_m - E_H\right) \; ; \quad \Gamma = \Gamma_0 \frac{\rho_0}{\rho} \; ; \quad U_s = c_0 + s\, U_p \qquad (2)$$

where p_H and E_H are, respectively, the Hugoniot pressure and the specific energy per unit mass, Γ is the Grüneisen ratio, Γ_0 a material constant, ρ_0 a reference density, U_s the shock velocity, U_p the velocity of a material point, c_0 the speed of sound and s a material

constant. Contact formulation was chosen as “Hard” for the normal part and “penalty’ for the tangential one

As in micro compression tests, a first impact simulation was performed with JC parameters taken from literature. The second one used A, B and n values from the quasi-static study (A=54.7 MPa, B= 98.9 MPa and n= 0.653). This part of the study is still on-going. Modeling results could be compared to experimental observations considering only splat diameter. In future developments, the kriging modeling approach already deployed for quasi-static analysis will be extended to the dynamic case and also splat morphology will be added to the fitting procedure.

The first result obtained by the combination of static and dynamic tests, despite some uncertainties in parameter fitting and the high ductility of the receiver substrate, seems to indicate that the powder tested has a softer behaviour than bulk aluminium, with a higher strain rate sensitivity. This must be confirmed by future tests and observations. Nevertheless, it is possible that, due to a particular setting of atomization conditions to obtain spherical particles, a lower solidification rate was responsible for a coarser microstructure than standard powder and then closer to bulk microstructure. In addition, the presence of Fe in the material, despite its low percentage, may be responsible for its softening. The mechanism is illustrated in in Fig. 7. Iron has a higher melting temperature than Al and is more soluble in liquid than in solid. With the fast cooling rate, it can be confined in the liquid phase by the advancing solidification front. Energy and time are not sufficient for iron to diffuse inside grains in solid state. This would result in iron segregation at the grain boundaries and in the formation of brittle intermetallic phases, such as Al_2Fe, Al_5Fe_2 or $FeAl_3$, usually present in alloys with more than 5%wt. Fe. According to [21], the mechanical behaviour of grain boundaries can strongly affect the mechanical properties of materials, explaining the possible softer behaviour of this Al powder. A deeper metallurgical characterization of the powder will be carried out in future works to verify this hypothesis

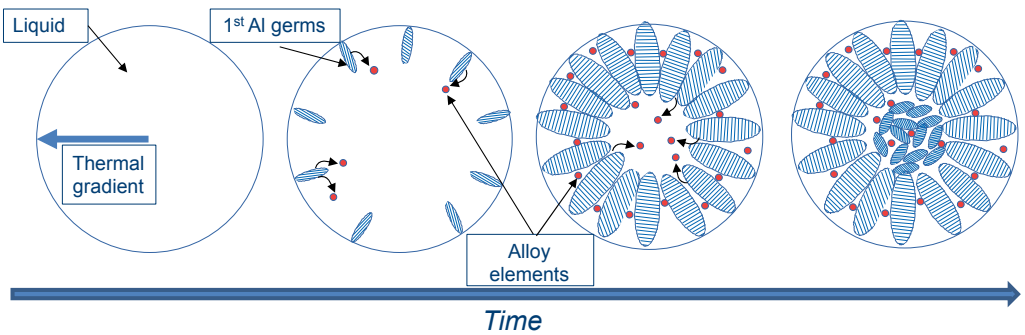

Fig. 7. S Schematic view of the mechanism occurring during particle solidification and bringing to the segregation of alloy elements at grain boundaries. Solid Al cellule nucleation and growth are shown in blue, alloy elements in red.

4 Conclusion and perspectives

In this study, a method for the mechanical characterization of powders was developed and applied to spherical aluminum. Cyclic micro-compression experiments in quasi-static regime were coupled with fast dynamic LASHPOL experiments, where single particles were accelerated to cold spray velocities. Numerical simulations of both tests were developed to fit material behavior parameters. Gathering results from static and dynamic experimental frameworks was shown to be a promising way to characterize material

behavior of powders in conditions similar to those encountered in cold spray. First results are promising but more work is still needed to validate the approach. The kriging fitting method must be studied in depth to investigate the uniqueness of the best fitting parameter set, as well as the influence of JC coefficient initial values. In future work, mechanical properties of different Al powders produced by TOYAL will be studied in correlation with microstructural characteristics, purity, atomization conditions and granulometry.
The LASHPOL platform achieved its principal goal of accelerating a single particle at measurable velocities in the cold spray range. Nevertheless, some further testing and improvements are still ongoing. The coupling between quasi-static and dynamic testing methods and simulations is a promising way to improve the mechanical characterization if powders. Results obtained so far are encouraging. Disposing of an accurate knowledge of powder mechanical behavior can be very valuable for both the end user and the powder producer. The first would be confirmed in the choice of the best powder for a given application and, the second, supported to find the best application for a given powder. Together, they can collaborate to tailor powder properties for better spraying performances. Another promising application field for powder mechanical testing concerns the development of alloyed powders suitable for cold spraying. These materials are known to be, sometimes, difficult to spray, probably due to excessive hardness. As suggested by some works, such as [3] and [22], powder heat treatment could be a viable way to modify the microstructure and increase its ductility. Nevertheless, the optimization of powder heat treatment can be a long and expensive process, involving numerous experimental tests and characterizations. Testing singles particles allows to compare direct numbers rather few data in various parameters process such as cold spray projection.

References

1. H. Assadi, H. Kreye, F. Gärtner, and T. Klassen, *Cold spraying – A materials perspective*, Acta Mater., **116**, pp. 382–407 (2016).
2. P. R. Sreenivasan and S. K. Ray, *Mechanical Testing at High Strain Rates,* in Encyclopedia of Materials: Science and Technology, Elsevier, pp. 5269–5271 (2001).
3. A. Sabard, H. L. de Villiers Lovelock, and T. Hussain, *Microstructural Evolution in Solution Heat Treatment of Gas-Atomized Al Alloy (7075) Powder for Cold Spray,* J. Therm. Spray Technol., **27**, pp. 145–158 (2018).
4. H. Jones, *Microstructure of rapidly solidified materials*, Mater. Sci. Eng., **65**, pp. 145–156, (1984).
5. S. Barradas et al., *Laser shock flier impact simulation of particle-substrate interactions in cold spray*, J. Therm. Spray Technol., **16**, pp. 548–556 (2007).
6. M. Hassani-Gangaraj, D. Veysset, K. A. Nelson, and C. A. Schuh, *In-situ observations of single micro-particle impact bonding*, Scr. Mater., **145**, pp. 9–13 (2018).
7. K. Sundberg et al., *Finite Element Modeling of Single-Particle Impacts for the Optimization of Antimicrobial Copper Cold Spray Coatings*, J. Therm. Spray Technol., **29**, pp. 1847–1862 (2020).
8. A. A. Dehkharghani, *Tuning Johnson-Cook Material Model Parameters for Impact of High Velocity , Micron Scale Aluminum Particles*, no. (2016).
9. H. Assadi et al., *Determination of plastic constitutive properties of microparticles through single particle compression*, Adv. Powder Tech., **26**, pp. 1544–1554 (2015).

10. G. R. Johnson and W. H. Cook, *Fracture characteristics of three metals subjected to various strains, strain rates, temperatures and pressures*, Eng. Fract. Mech., **21**, pp. 31–48 (1985).
11. D. L. Preston, D. L. Tonks, and D. C. Wallace, *Model of plastic deformation for extreme loading conditions*, J.Appl.Phys. **93**, pp. 211–220 (2003).
12. S. Rahmati and B. Jodoin, *Physically Based Finite Element Modeling Method to Predict Metallic Bonding in Cold Spray*, J Therm Spray Tech, **29**, pp. 611–629 (2020).
13. A. Fardan, C. C. Berndt, and R. Ahmed, *Numerical modelling of particle impact and residual stresses in cold sprayed coatings: A review,* Surface and Coatings Technology, **409**. (2021).
14. D. Garcia-Gonzalez, R. Zaera, and A. Arias, *A hyperelastic-thermoviscoplastic constitutive model for semi-crystalline polymers: Application to PEEK under dynamic loading conditions*, Int. J. Plast., **88**, pp. 27–52 (2017).
15. M. Liu and H. Proudhon, *Finite element analysis of contact deformation regimes of an elastic-power plastic hardening sinusoidal asperity*, Mech. Mater., **103**, pp. 1339–1351 (2016).
16. G. Johnson, *Material characterization for warhead computation*, Prog. Astronaut. Aeronaut., **155**, pp. 165–197 (1993).
17. S. Sahu et al., *Finite element analysis of AA1100 elasto-plastic behaviour using Johnson-Cook model*, Mater. Today Proc., **5**, pp. 5349–5353 (2018).
18. T. Hussain et al., *Materials Science and Technology Bonding between aluminium and copper in cold spraying: story of asymmetry Bonding between aluminium and copper in cold spraying: story of asymmetry*, Materials Science and Technology, **28**, pp. 1371-1378 (2012).
19. V. K. Champagne et al.,, *The effect of cold spray impact velocity on deposit hardness*, Model. Simul. Mater. Sci. Eng., **18**, (2010)
20. S. Weiller, F. Delloro, P. Lomonaco, M. Jeandin, and C. Garion, *A finite elements study on porosity creation mechanisms in cold sprayed coatings,* Key Eng. Mater., vol. 813 KEM, pp. 358–363 (2019).
21. T. Watanabe and S. Tsurekawa, *Control of brittleness and development of desirable mechanical properties in polycrystalline systems by grain boundary engineering*, Acta Mater., **47**, pp. 4171–4185 (1999).
22. A. Sabard and T. Hussain, *Bonding mechanisms in cold spray deposition of gas atomised and solution heat-treated Al 6061 powder by EBSD*, arXiv, 2018.